DOI 10.5162/ETTC2024/A1.1

The Use of Lidar to Measure the Flexion and Torsion of a Wing

Israel López Herreros[1,3], Felix Arevalo Lozano[1], Jesús Barrera Rodríguez[1], Andrés Egido Fernández[1], Marcos Chimeno[2], Pablo García-Fogeda Núñez[2]
[1] Airbus Defence and Space, John Lennon S/N 28906 Getafe-Madrid, Spain
[2] Department of Aircraft and Space Vehicles, ETSIAE, Universidad Politécnica de madrid, Madrid, Spain
[3]israel.lopez@airbus.com

Abstract:
In the field of aerospace, photogrammetry is one of the traditional technologies used to monitor deformations in components such as aircraft wings or other structures, providing valuable data for structural design and evaluation. For these kind of use cases normally two synchronized cameras are needed, they have to be separated by a certain distance to ensure good triangulation.

The current challenge is to assess a new testing technology something less intrusive and less time-demanding in post-processing than photogrammetry methodology. Lidar-based techniques emerge as promising alternatives. Airbus Defence and Space has evaluated the lidar for in-flight relative positioning between two aircrafts, acquiring the knowledge, advantages, and disadvantages of this technology. The objective is to assess this new sensor to measure the flexion and torsion of a wing.

This paper will explain the methodology applied to the point cloud coming from the lidar to characterize the deformation of a wing. Fusion with camera image, clustering algorithms and vibration analysis will be fundamental elements of this process. Simulation and ground tests on a wing mockup will be used to validate the methodology and will allow to choose the best configuration before flight tests.

Key words: lidar, wing deformations, flexion, torsion

1. Introduction

In the field of aerospace, photogrammetry is one the traditional technology used to monitor deformations in components such as aircraft wings or other structures, providing valuable data for structural design and evaluation. For these kind of use cases normally two synchronized cameras are needed, they have to be separated by a certain distance to ensure good triangulation. In some cases irregular dot pattern stickers are used. Applying this methodology in big wings is not an easy task [1].

The current challenge is to assess a new testing technology something less time-consuming in post-processing than photogrammetry methodology. Lidar-based techniques emerge as promising alternatives. Airbus Defence and Space has evaluated the lidar for in-flight relative positioning between two aircrafts [2], acquiring the knowledge, advantages, and disadvantages of this technology. The objective is to assess this new sensor to measure the flexion and torsion of a wing.

2. Lidar

A modern lidar functions by scanning its surroundings with one or more laser beams, which are steered precisely to cover its field of view and that are reflected by the environment back to the scanner. These reflections are transformed into electronic signals by a photodetector, which are then filtered and processed. A 3D point cloud corresponding to the scanned environment as well as the intensities of the reflected beams constitute the output of a lidar system (see Fig. 1). Such a system can be divided into two main components:

- The laser rangefinder: which comprises the laser transmitter, collimated by optics that is shone on the target; photodetector, that generates an electronic signal from the reflected photons that are focused on it by optical elements; and signal processing electronics for estimating the distance between sources and reflecting sources.

- The scanning system: which typically steers the laser beam, following different azimuths and vertical angles. This element defines the system's field of view.

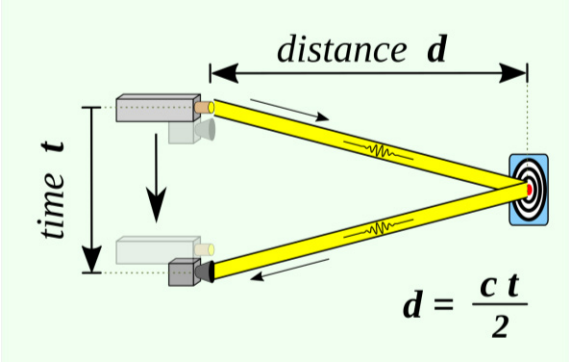

Fig.1. Lidar technological principles

3. Lidar Use Case

The aircraft models used to calculate loads and aeroelastic instabilities need to be validated with ground and flight tests. The most important ground test to obtain the stiffness properties of the aircraft flexible structure is the Ground Vibration Test (GVT). On the other hand, the Flight Vibration Test (FVT) is the most relevant test to characterize the in-flight aircraft flexible response. The FVT is mainly focussed on the transient response of the structure subjected to control surfaces rotations (ailerons, elevators or rudder) and the main objective is to assess that the aircraft, as a system, does have positive damping. The FVT instrumentation is reduced (telemetry-related restrictions) and mainly based on accelerometers located on fuselage and tips of lifting surfaces (wing, HTP, and VTP) and, although the response is well captured in terms of frequency and damping, the deformation shape is hardly characterized with only this instrumentation. Lidar-based techniques could be used to complement the information coming from the FVT, giving additional information as the in-flight steady deformation or the in-flight transient motion due to external perturbations. The lidar-based tools are non-invasive and, with a reduced cost, could be developed to obtain valuable information on the aircraft flexible deformation.

In fact, a prototype beta version of the hardware and software described in this paper will be on-board of an A330-MRTT of Airbus Defence and Space (Airbus-DS) to measure wing elastic deformation, with emphasis on obtaining the local translations/rotations of the underwing refuelling pods (see Fig. 2).

After these tests, future evolutions of this technology are intended to be applied on subsequent prototypes of Airbus-DS.

Fig. 2. A330-MRTT aircraft refuelling two fighters through the underwing pods

3.1 Mockup Properties, Design, and Manufacturing

A mockup with a high aspect ratio has been manufactured using a 3D printer. The objective was:

1. Create a model to represent the new developments in high aspect ratio wings aimed to reducing emissions while providing high lift/drag ratios.
2. Ensure that the model has a low first bending eigenfrequency for future investigation into the aeroelastic behaviour due to geometrical nonlinearities in the vibration of the mockup.

The mockup has the following geometrical properties:

- Aspect ratio: 18
- Air foil section NACA 4414
- Taper ratio 0.65
- Half span b/2 1m
- Root chord c_r 0.1347m
- Tip chord c_t 0.0875m

A sketch of the wing model can be seen at the fig. 3.

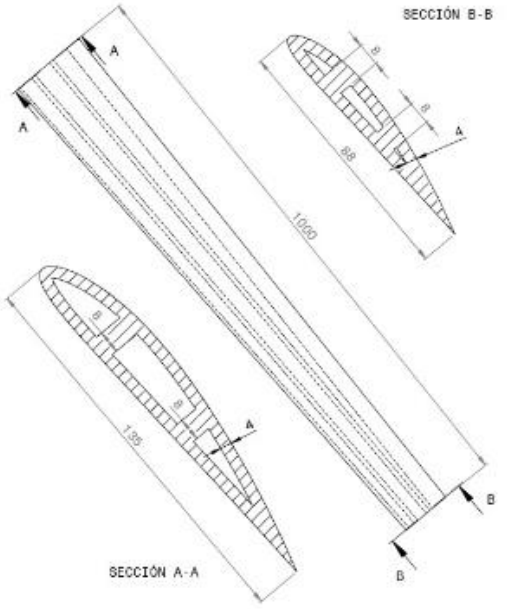

Fig. 3. Wing model

The printing material used was polylactic acid (PLA), a biodegradable thermoplastic polyester produced from renewable sources. It is characterized by a low melting point, a low coefficient of thermal expansion, as well as high flexural strength. The nominal properties of PLA are as follows:

- Elastic modulus E [GPa] 2.5
- Density [kg/m^3] 1250
- Poisson's ratio [-] 0.36

However, the experience acquired from previous bending tests on segmented, 3D-printed, and assembled beams has revealed a change in the mechanical properties of the printing material during the printing process. Therefore, an empirically determined value of E=1.75GPa (approximately 70% of the filament's nominal Elastic modulus) must be used henceforth for the analysis of the mockup. This adjusted value has been validated through mechanical tests performed on the mockup post-manufacturing.

The first bending frequency of the model is of 4hz, which is considered low enough for conducting studies related to the second objective.

3.2 Structural Model

In order to have an additional comparison against lidar results, a Finite Element Model (FEM) of the mockup structure has been built and computations of static and dynamic tests have been performed. This model has been defined with the same data (geometry, materials, etc.) which were stated in section 3.1 using quadrilateral 2D elements with shell properties ("CQUAD4" and "PSHELL" in NASTRAN notation). Additionally, a structural damping of g=2.7% has been considered to take into account the decaying response after release. This coefficient has been estimated with the results from the analysis of the accelerometers during the dynamic tests.

Three kinds of analyses have been carried out with this model:

- Linear static (SOL 101): to obtain the static deformation under the own weight of the mockup plus the additional mass at the wing tip
- Modal analysis (SOL 103): to check the eigenfrequencies and modes of the structure before dynamic analysis.
- Modal transient response (SOL 112): to compute the dynamic response after the release of the wingtip load.

Tab. 1 registers the first eigenfrequencies of the model whereas fig. 4 shows the static deflection of the full model under its own weight and a 200g mass located at its wingtip.

n	Frequency [Hz]	Mode description
1	3.82	1st bending mode
2	19.29	2nd bending mode
3	23.28	1st for-aft mode
4	50.16	3rd bending mode
5	67.92	1st torsion mode

Tab. 1. First eigenfrequencies of the model

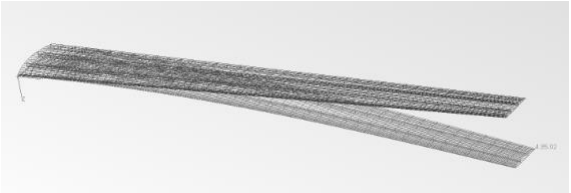

Fig. 4. Full model static deformation

3.3 Tests Requirements

In order to validate the feasibility of the lidar-based techniques to experimentally characterize the deformation of wing-like flexible structures ground tests are requested. The text specimen for the ground test is the wing mockup explained in the previous sections.

Two types of ground tests are requested:

- Static tests: Intended to cause a static deformation of the mockup due to the addition of calibrated masses at the wing tip. Two positions along the wing chord are specified for getting both pure bending deformation and bending + torsion deformation.
- Dynamic tests: Intended to force a dynamic response of the mockup due to the release of a calibrated mass stored at the wing tip. Four lidar sampling frequencies (10, 16, 24 and 30hz) are requested to characterize the dynamic response of the mockup.

All the steps of the planned test sequence are summarized in the following table:

Test Case	Excitation Method	Excitation Point	Mass	Sampling Frequency
0	N/A	N/A	N/A	SP1: 1 Hz
1	Static Load	EP1 (Bending)	50 g	
2	Static Load		100 g	
10	Static Load		150 g	
3	Static Load		200 g	
4	Static Load	EP2 (Bending and Torsion)	50 g	
5	Static Load		100 g	
6	Static Load		200 g	
7	Load Release	EP1 (Bending)	200 g	SF2: 10 Hz
8	Load Release			SF3: 16 Hz
12	Load Release			SF4: 24 Hz
9	Load Release			SF5: 30 Hz

Tab.2. Planned test sequence

4. Lidar Methodology

This section will explain the lidar-based methodology to measure the flexion and torsion of a wing. The output from this methodology will be a time history with several positions of the wing. The following stages will be applied for each frame:

4.1 Point cloud recovery

The first step of the pipeline consists of obtaining the raw point cloud corresponding to the current frame where the wing should be within the lidar's field of view (see Fig. 1).

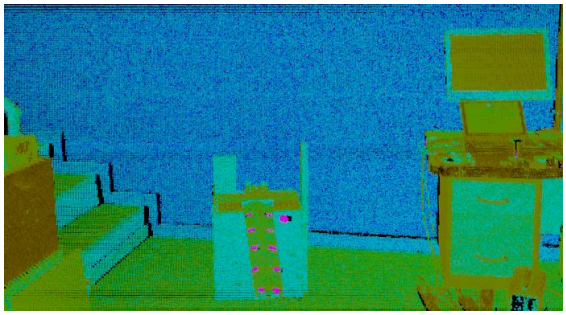

Fig. 5. Point cloud of the wing mockup

4.2 Filter by reflectance

Reflective stickers will be used to filter the point cloud and keep the relevant information. Most of the point cloud disappears, this speeds up the rest of the stages (see Fig. 6).

Fig. 6. Point cloud filtered by reflectance

4.3 Filter by geometry

A geometry filter will be used to remove points outside of the wing (see Fig. 7).

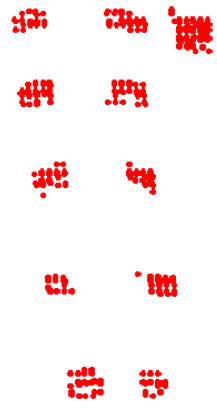

Fig. 7. Point cloud filtered by geometry

4.4 Clustering

A density-based algorithm for discovering clusters in large spatial databases with noise is applied in this stage. Two parameters will have to be adjusted:

- eps: specifies how close points should be to each other to be considered a part of a cluster.
- minimum points: Minimum number of points to form a cluster

These two parameters should be taken into account in the arrangement of the stickers. On one hand, if two stickers are very close it may not be possible to generate two clusters. On the other hand, if the stickers are too far from the lidar it may lead to not having enough points to define properly a cluster.

Each cluster will play the role of a position sensor to characterize the wing deformation (see Fig. 8).

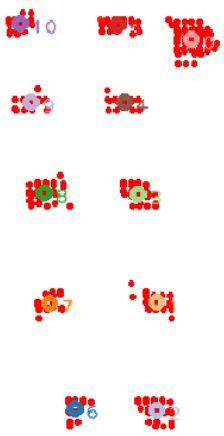

Fig. 8. Clusters of the wing mockup

4.5 Filter by size

When the wing is moving the clusters can significantly vary their geometry producing some noise in the cluster position. To protect this kind of situations a size-based filter is applied. The clusters will need to have a geometry similar to the sticker.

4.6 Centroid calculation

For each cluster, its position will be calculated as the mean of the points that compose it.

4.7 The coherence of the clusters

The density-based algorithm does not have history, that means that the clusters from one frame are not related to the clusters of the following frame. A Neighbourhood-based algorithm is applied to maintain the coherence of the clusters. A maximum cluster displacement is used. This parameter has to be adjusted for the use case.

4.8 Surface reconstruction

To interpretate the resulting point cloud correctly it is very useful to stich the points to form a mesh. A surface reconstruction algorithm is applied in this stage (see Fig. 9).

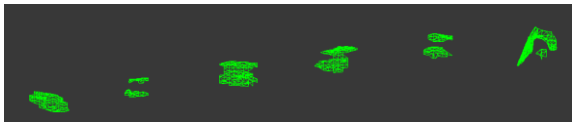

Fig. 9. Mesh generation for each cluster

4.9 Position of the clusters respect to a reference

To characterize the wing deformation is very useful to compare the deformation against other deformations. In this stage each cluster position will be calculated relative to a cluster reference.

The main output from this pipeline is the time series with the position of the clusters. There are some small gaps in the signal that will be reconstructed using interpolations (see Fig. 10).

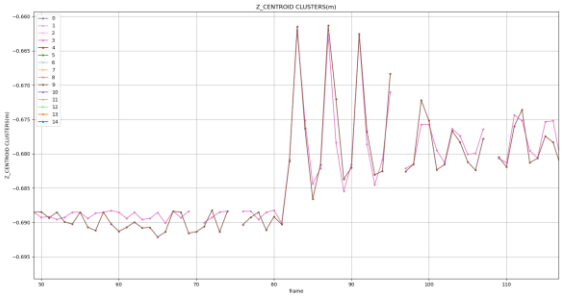

Fig. 10. Time series with the position of the clusters

A vibration analysis based on power spectral density (see Fig. 15) and spectrograms is applied to these signals to obtain the vibration modes lower than half of the lidar sampling rate according to the Nyquist theorem.

5. Test Means

The following means were used to execute the tests.

5.1 Laser distance meter

Used to measure with high accuracy (+-1.5mm) the height of the stickers during the static tests (see Fig. 11).

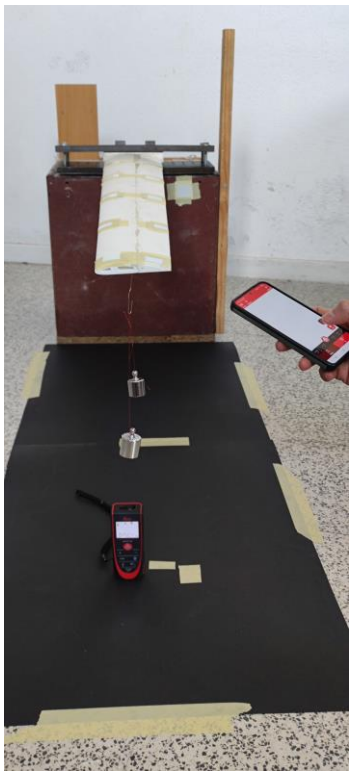

Fig. 11. Laser measurements

5.2 Lidar

Used to measure (range precision < 2cm 1σ, 50m) the 3D position of the stickers during the static and dynamic tests. The maximum number of horizontal lines are 640 at 1hz. This number of lines is inversely proportional to the rate, it means that if the rate is 10hz the maximum number of horizontal lines will be 64. Therefore the lidar resolution decreases with the rate.

5.3 Reflective stickers

Reflective stickers will be used to filter the point cloud and keep the relevant information (see Fig. 11).

5.4 Accelerometers

For the dynamic tests, accelerations at the ten locations of the reflective stickers were measured by means of piezoelectric accelerometers. The sensors were installed in the lower surface of the wing to avoid interfering in the cloud point processing (see Fig. 12).

Fig. 12. Accelerometers in the lower surface to measure the dynamic tests response

The accelerations were measured by a set of CCLD Bruel & Kjaer accelerometers acquired through a LDS Dactron Focus II system with a time resolution of $3.9 \cdot 10^{-3}$s in the time domain and 0.125hz in the frequency domain.

6. Test Execution and validation

Following sections present the tests results obtained with the different sources. Static torsion tests will not be presented because the effect on the wing is negligible.

6.1 Static results

Static test T0 (0g) will be used as the reference for the rest of the static tests. Several static loads were performed with increasing load at the wing tip: 50gr (T1), 100gr (T2), 150 gr (T3) and 200gr (T4).

T4 analysis will be displayed in this paper for producing the most severe deformation. Similar results were found in T1, T2 and T3. Fig. 13 shows the displacement of the wing in the z-axis respect to the reference during the static tests T4 (200g). There are four series corresponding to the different sources: Nastran model in blue, laser data in orange, lidar data in purple and the integration from the accelerometers in red. The orange zone outlines the laser's confidence band.

The purple zone outlines the lidar's confidence band necessary to make the lidar data compatible with the rest of the sources. In this case use the precision of the methodology using the lidar is 2.5mm.

There are some discrepancies among the different sources but they all have a similar trend.

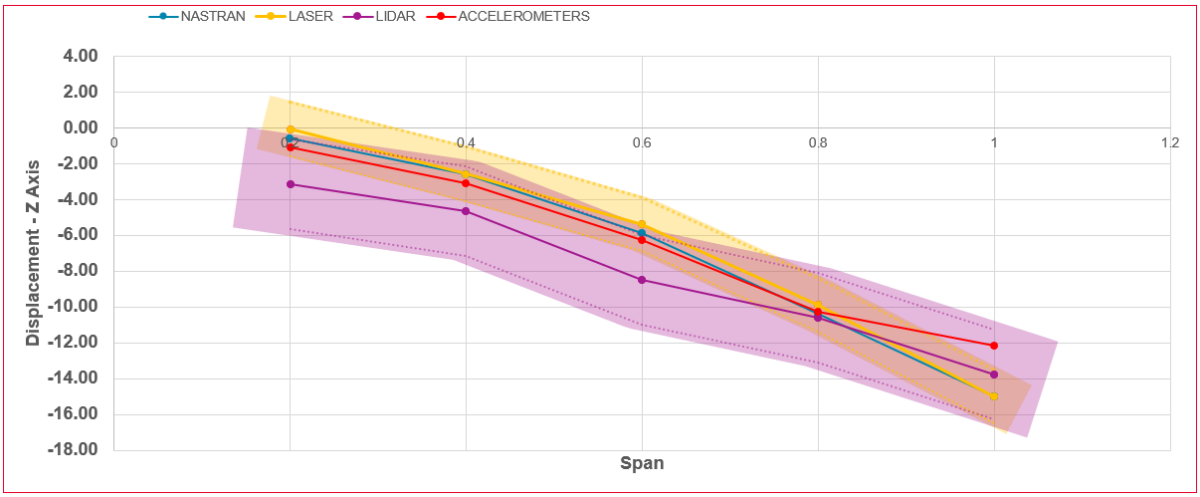

Fig. 13. Wing deformation with static load of 200g

6.2 Dynamic Results

The 200g load release test has been repeated with the following lidar sampling: 10, 16, 24 and 30hz. The ideal lidar configuration for these dynamic tests is the one that has maximum sampling without losing the cluster identification. In this use case the best sampling has been at 16hz.

Fig. 14 shows the oscillations at the wingtip in the z axis during the test T8 (16hz). There are three sources of data: lidar in blue, Nastran in yellow and the integration from the accelerometers in black. The structural damping coefficient (g) in the Nastran model has been re-estimated using the accelerometer data because it has more precision that the lidar.

Maximum amplitude and damping are coherent in the different sources, however the lidar data has a higher level of noise due to its calculation methodology.

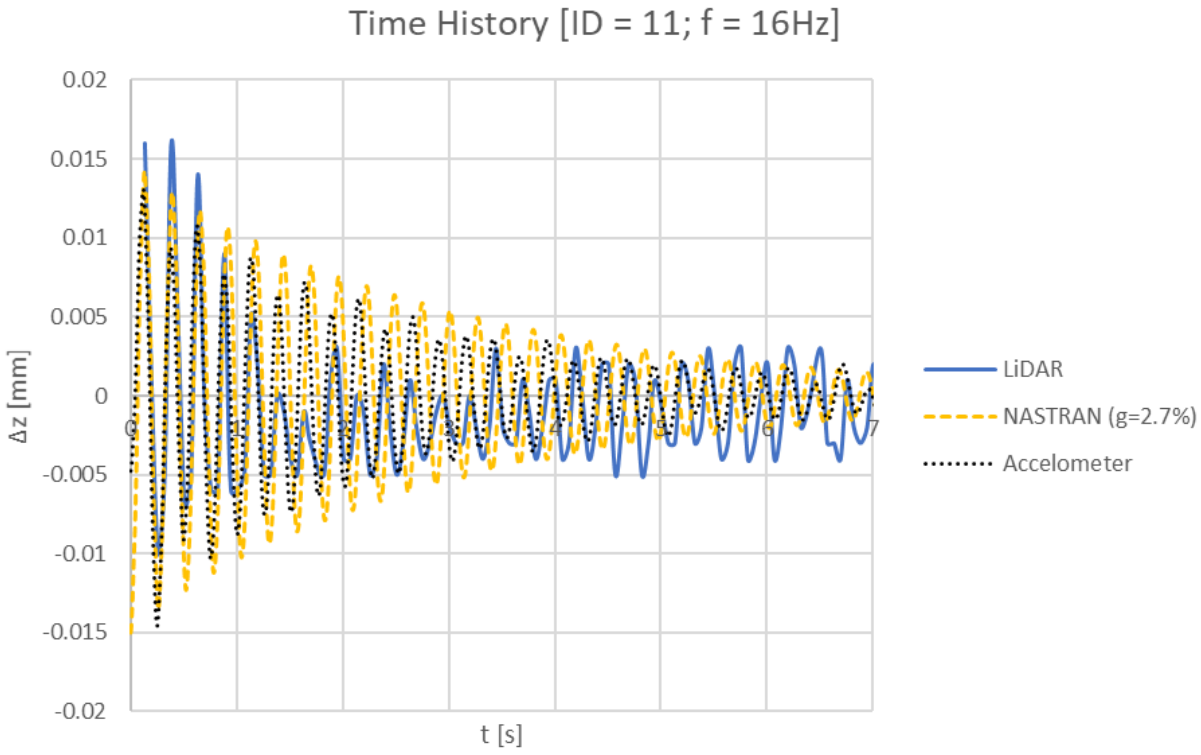

Fig. 14. Dynamic test lidar (16hz)

The power spectral density is applied to the different sources obtaining a similar frequency in the wingtip (see Fig. 15, 16 and 17). The dynamic response is coherent with the first bending mode (See Table 1). The limited lidar sampling rate does not allow identifying other vibration modes.

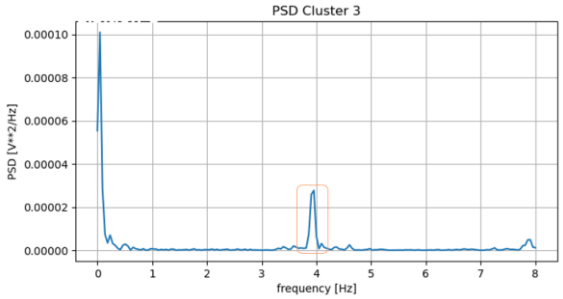

Fig. 15. Lidar PSD wingtip (16hz)

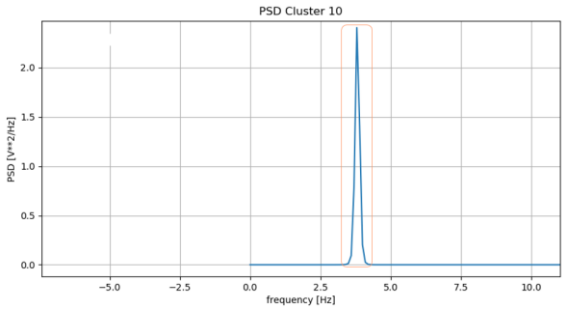

Fig. 16. Nastran PSD wingtip (2000hz)

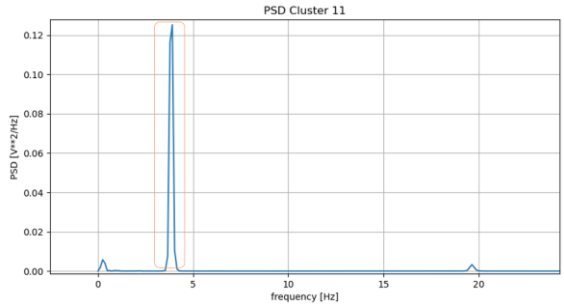

Fig. 17. Accelerometers PSD wingtip (250hz)

7. Conclusions

This lidar-based methodology is applied to measure the flexion and torsion of a wing mockup wing in static tests with a precision of 2.5mm.

For dynamic tests, the lidar sampling rate chosen was 16hz for having maximum sampling without losing the cluster identification. This limits the identification just to the first 4hz vibration mode of the wing mockup, therefore the analysis is restricted to this mode.

This work has been done with a specific lidar coming from the automotive sector. Currently, lidars are seen as a key ingredient to autonomous driving. In the future, lidars with better performance in terms of precision, range, and sampling are expected to be available.

This work paves the way to the use of the lidar technology to measure the flexion and torsion of the wing of a real aircraft or any other structure. This methodology could be also applied to measure structure deformations in ground tests.

Acknowledgement

I'd like to acknowledge the contribution of Francisca Coll Herrero to support the implementation of the vibration analysis.

References

[1] F. Boden, T. Kirmese, T. Weikert, T. Wofl, C. Petit, H. W. Jentink: "Application of a new optical measurement technique for non-intrusive wing deformation measurements on a large transport aircraft", SFTE 2010

[2] Israel López Herreros: "Lidar for in-flight accurate relative positioning", ETTC 2023

Glossary

LIDAR: Light Detection and Ranging
GVT: Ground Vibration Test
FVT: Flight Vibration Test
HTP: Horizontal Tail Plane
VTP: Vertical Tail Plane
MRTT: Multi-Role Tanker Transport
DS: Defence and Space
PLA: PolyLactic Acid
PSD: Power Spectral Density